Polymer Degradation and Stability 126 (2016) 159–169

Contents lists available at ScienceDirect

Polymer Degradation and Stability

journal homepage: www.elsevier.com/locate/polydegstab

In vitro degradation of electrospun poly(L-lactic acid)/segmented poly(ester urethane) blends

Florencia Montini-Ballarin, Pablo C. Caracciolo, Guadalupe Rivero, Gustavo A. Abraham*

Research Institute for Materials Science and Technology, INTEMA (UNMdP-CONICET), Mar del Plata, Argentina

ARTICLE INFO

Article history:
Received 15 October 2015
Received in revised form
3 February 2016
Accepted 11 February 2016
Available online 13 February 2016

Keywords:
Hydrolytic degradation
Electrospinning
Bioresorbable polymers

ABSTRACT

Scaffold degradation behavior is one of the main aspects to be considered in tissue engineering applications. The hydrolytic *in vitro* degradation of compliant biomimetic electrospun bilayered vascular grafts made of poly(L-lactic acid) and segmented poly(ester urethane) blends was studied. Two polymeric blends were selected based on the natural arteries collagen and elastin composition, structure and functionality. The variation of molecular weight, and thermal and surface properties of the blends and their plain polymers, were analyzed and related to the structural and morphological changes taking place during degradation. The low initial crystallinity and high hydrophilicity of the blends, along with a synergetic outcome produced by blending, led to a higher molecular weight loss. Even more, it was observed that a bilayered graft made from these blends would degrade evenly as a whole. Moreover, the degradation time was found to match with the required for the regeneration processes. These facts make them encouraging for a future application as degradable small-diameter vascular constructs.

© 2016 Elsevier Ltd. All rights reserved.

1. Introduction

Tissue engineering emerged as a multi- and interdisciplinary approach to overcome the limitations of traditional therapies for the treatment of organ failure or replacement. When considering tissue engineering classical paradigm, a biomaterial is typically used in the form of scaffold, which brings the final form of the regenerating tissue and provides biological and mechanical signals. Artificial extracellular matrices (ECMs), among other properties, have to be bioresorbable. They carry out a temporary function and permit the production of natural ECMs by the implanted or migrated cells. Therefore, biocompatibility, degradation rate and material properties evolution during its degradation are crutial factors in tissue engineering, since they influence the cellular behavior, tissue growth, local homeostasis and biomechanical microambient. Ideally, the scaffold degradation rate should be synchronized with the tissue regeneration rate, i.e. go along with the tissue growing process [1–3].

Polymers degradation rate depends on various parameters closely related to their degradation mechanism, as the molecular weight, polydispersity, crystallinity, crystal orientation and morphology, and glass transition temperature [4–6]. Polymer blends offer a simple means of combining the properties of two materials to achieve a new one. Blending two polymers with different degradation profiles may serve as a strategy to achieve a desirable rate of degradation [7–10], or to tune physical, mechanical or surface properties [11–14]. For the former case, the composition and microstructure of the present phases as well as the miscibility and compatibility of the blended components are key parameters influencing the resulting degradation rate.

Aliphatic polyesters, such as poly(ε-caprolactone) (PCL), poly(L-lactic acid) (PLLA) and poly(glycolic acid) (PGA), as well as their copolymers and blends, are approved by U.S. Food and Drug Administration (FDA) and usually chosen as synthetic biodegradable polymers for tissue engineering applications. These biocompatible polymers present a semicrystalline structure and good electro-spinnability [15,16]. Among them, PLLA has a mechanical response similar to collagen [17], with a high elastic modulus required to withstand high pressure and stresses, thus preventing collapse or degradation until the tissue develops and matures *in vivo*. Its degradation process occurs by hydrolysis, leading to a decrease in the macromolecules average length when water reacts with the ester unions present in the polymeric chains [18–20]. This process involves different stages. Firstly, the amorphous regions react with water molecules since their segments are more flexible.

* Corresponding author. INTEMA (UNMdP-CONICET), Av. Juan B. Justo 4302, B7608FDQ Mar del Plata, Argentina.
E-mail address: gabraham@fi.mdp.edu.ar (G.A. Abraham).

http://dx.doi.org/10.1016/j.polymdegradstab.2016.02.007
0141-3910/© 2016 Elsevier Ltd. All rights reserved.

This leads to an increase in chain mobility that reorganizes in new more defective crystals. Secondly, the degradation rate can be accelerated because of the autocatalytic effect caused by the acidic nature of the generated carboxylic end-groups. Finally, hydrolysis takes place at the crystalline regions. Cha et al., Hiljanen-Vainio et al., and Gaona et al. studied different strategies for tailoring PLLA degradation rates when blended with PCL, poly(glycolic acid-co-L-lactic acid) (PGLA), and poly(ε-caprolactone-co-L-lactide) (PCL/LLA) polyesters [8,9,21].

Segmented polyurethane (SPU) thermoplastic elastomers consisting of alternating soft and hard segments can be designed to obtain excellent mechanical properties, such as tensile strength and good compliance, and biocompatibility [22,23]. Considering mainly their viscoelastic compliant nature, SPUs provide an elastin-like mechanical behavior [24,25]. Taking advantage of this nature, and also the possibility to fine tune their degradation behavior (based on the degradation mechanism and rate), the precise design and use of bioresorbable SPUs for soft tissue engineering was encouraged [26]. Soft segments are usually employed to introduce chemical bonds susceptible to degradation, and therefore customize the material degradation rate. Oppositely, hard segments are often degraded through enzymatic mechanisms. Although degradation mechanisms depend on both the SPU soft and hard segments, there are certain mechanisms common to the majority of bioresorbable polyurethanes. In general, ester bonds are hydrolyzed in α-hydroxy acid oligomers as degradation products, as well as in fragments containing urethane and urea with acid terminal groups. The composition of the prepolymer or macropolyol has shown to control the *in vitro* degradation rate [23]. When soft segments are composed of ester derivatives, the degradation process is mainly the same as the one mentioned before for PLLA. It has been observed that SPUs with amorphous soft segments degrade faster than others with semicrystalline soft segments. Additional degradation of urethane and urea groups to free polyamines could take place, depending on the used diisocyanate [23].

Electrospinning emerged as a versatile processing technology to obtain porous structures with high surface to volume ratio that mimics the natural ECM. The technique allows the formation of different fiber morphologies and orientations, as well as geometries such as tubular structures for vascular tissue engineering. It was reported that electrospun structures exhibit different thermal, surface, and mechanical properties compared to their bulk counterparts [27–29]. Even more, the nanofibrous structure could also influence the polymer degradation rate. It was reported that porous materials or thin films exhibit a slower degradation rate than their thick bulk counterparts. It is believed that the degradation products with acid terminals can diffuse easily through these materials, leading to an absence of autocatalytic effect. On the other hand, a nano-object which consists of only a few polymeric chains and presents a high area to volume relation, should present a faster degradation rate. Thus, the degradation rate for nanostructured materials is the result of a competition between both effects [21,30]. Some groups studied the hydrolytic degradation process of nanofibrous membranes based on electrospun polyesters, polyurethanes and some polyester blends [18,19,30–35]. However, these works were focused almost exclusively on the mechanism of degradation and the scaffold stability of plain polymer nanofibers. Moreover, when blending was performed to tailor the degradation rate, their behavior evaluation was limited to short periods of time (up to 7 weeks) [10,18,32].

PLLA, a segmented poly(ester urethane) (SPEU), and their blends, were previously considered in our group for vascular tissue engineering applications. The blend ratios were chosen in order to mimic the structure of natural arteries media and adventitia layers and their characteristic mechanical response; bilayered vascular grafts were developed [36]. These grafts exhibited a compliant biomimetic performance and an excellent behavior under physiological condition [17,37–40]. To the best of our knowledge, the effect of blending PLLA and a SPEU on their degradation behavior has not been reported before. Thus, the hydrolytic degradation of these materials is studied in this work. Moreover, the time scale of the assay was foreseen in accordance to the vascular tissue regeneration rate. The variations on thermal and surface properties were studied and related to the structural and morphological changes taking place during degradation.

2. Materials and methods

2.1. Materials

PLLA (PLA2002D Mn = 78.02 kg mol^{-1}, Mw = 129.91 kg mol^{-1}, IP = 1.67, 99.6% L-lactic acid sequences, and a 37.6% crystallinity degree) was obtained from Natureworks, MN, USA). PHD, a bioresorbable SPEU was synthesized in our laboratory. Dichloromethane (DCM) and *N*,*N*-dimethylformamide (DMF) were acquired from Anedra (BA, Argentina). Tetrahydrofuran (THF) was purchased from Cicarelli (Santa Fe, Argentina). 2,2,2-trifluoroethanol (TFE) was purchased from Sigma-Aldrich (MO, USA). All solvents were analytical grade and were used as received.

2.2. Methods

2.2.1. Synthesis of segmented poly(ester urethane) PHD

PHD was synthesized from an aliphatic diisocyanate, an aliphatic polyester, and a novel aromatic chain extender according to previously reported procedures [25]. Briefly, PCL diol (Mn = 2.250 kg mol^{-1}) was prepared by ring opening polymerization of ε-caprolactone initiated by triethylene glycol. A tyrosine derivative was used as diester–diphenol chain extender. This compound was synthesized by a Fischer esterification reaction between 3-(4-hydroxyphenyl)propionic acid (desaminotyrosine) and ethylene glycol (2:1 mol ratio) catalyzed by *p*-toluene sulfonic acid in refluxing toluene. The reaction was driven toward completion by using a Dean-Stark apparatus to trap the evolved water. PHD was obtained by a two-step polymerization method. Briefly, PCL diol was reacted with HDI in a 1:2.01 M ratio at 80 °C in anhydrous *N*,*N*-dimethylacetamide (DMAc) under stirring and nitrogen atmosphere. The prepolymerization reaction proceeded in presence of dibutyltindilaurate as catalyst (0.1% wt of macrodiol) for 1 h, and then the solution was concentrated. The chain extender was previously dissolved in DMAc and added at a molar ratio 1:1 with respect to the prepolymer. Chain extension reaction proceeded for 6 h at 80 °C. The resulting slurry was precipitated over cold distilled water. Then, the polymer was washed and dried under vacuum. The number average (Mn) and the weight average molecular weight (Mw), as determined by gel permeation chromatography (GPC), were 25.16 kg mol^{-1} and 58.47 kg mol^{-1} respectively, and the polydispersity index (PI) was 2.32.

2.2.2. Electrospinning

Small-diameter electrospun tubular structures were obtained according to previously reported conditions [36]. Tubular scaffolds were prepared from PLLA, PHD and two different blends of PLLA/PHD with 90/10 and 50/50 wt/wt ratio, named B90/10 and B50/50, respectively. B90/10 blend was selected to mimic natural arteries adventitia layer, whereas B50/50 blend intended to mimic the media layer. In this way, a bilayered vascular graft with an outer and inner layer composed of B90/10 and B50/50, respectively, was prepared [36]. The electrospinning setup includes a programmable syringe pump (Activa A22 ADOX S.A., Argentina) to control the flow

rate, a high-voltage power source (ES30P, Gamma High Voltage Research Inc.), and a grounded auxiliary aluminum collecting plate. A small-diameter rotating mandrel was used to collect the nanofibers. All experiments were carried out at room temperature in a chamber with a ventilation system. A 10% wt/v solution concentration (C) in DMF/DCM at 40/60 ratio, a voltage (V) of 13 kV, a needle-to-collector distance (d) of 15 cm, a flow rate (f) of 0.5 mL/h, and a rotational velocity (r) of 1000 rpm were used for the preparation of PLLA scaffolds. A PHD solution in TFE at C = 25% wt/v was processed at V = 13 kV, d = 15 cm, f = 1 mL/h, and r = 1000 rpm to prepare PHD scaffolds. A total C = 20% wt/v in TFE was used for B50/50, and 15% wt/v in TFE for B90/10. The electrospinning parameters used were V = 13 kV, d = 15 cm, f = 1 mL/h, and r = 1000 rpm for B50/50; and V = 13 kV, d = 15 cm, f = 0.5 mL/h, and r = 1000 rpm for B90/10.

2.2.3. in vitro hydrolytic degradation

The hydrolytic degradation of electrospun grafts based on PLLA, PHD, and B50/50 and B90/10 blends was studied *in vitro* during 34 weeks. Slices of approximately 10 mg were cut and placed in vials containing 5 mL of phosphate buffer solution (PBS, pH = 7.4). PBS was prepared from NaCl 0.137 mol L^{-1}, KCl 0.0027 mol L^{-1}, Na_2HPO_4 0.01 mol L^{-1}, KH_2PO_4 0.0018 mol L^{-1} and NaN_3 0.05% wt/v. Samples were incubated at 37 ± 1 °C and taken out at 1, 2, 3, 5, 8, 16, 24 and 34 weeks. pH was measured after each sample extraction and kept between 7.4 ± 0.5.

2.3. Characterization

2.3.1. Gel permeation chromatography (GPC)

PLLA and PHD average molecular weights (M_w, M_n) and polydispersity index (PI) were determined by gel permeation chromatography (GPC) at each degradation time. A chromatograph (Waters, Special Solvents (DMA) Empower Software) equipped with a refractive index detector (2414 Waters), and a three-column-arrangement (Polymer Standards Services GPC: 1 X GRAM Analytical 30 Å, 10 μm; and 2 X GRAM Analytical 1000 Å, 10 μm) at 35 °C was used. Poly(methyl methacrylate) (PMMA) standards were used for calibration. DMAc with LiBr (0.42 g/mL) was used as elution solvent. Studies were performed at 1 mL/min flux rate, with a 0.25 mg/mL concentration, and a 100 μL total volume. The molecular weight variation was expressed as relative molecular weight (M_{nr}), according to equation (1),

$$M_{nr} = (1 - (M_{n0} - M_{nt})/M_{n0}) * 100 \quad (1)$$

where M_{nt} indicates the molecular weight at a given time and M_{n0} is the molecular weight before degradation. When analyzing the molecular weight of the polymer blends, PLLA and PHD elution peaks were overlapped, therefore their deconvolution was not possible. Consequently, the peak corresponding to both PLLA and PHD was analyzed as a whole, and apparent M_n, M_w and PI were determined. Their variation over degradation time was analyzed in a similar way.

2.3.2. Fourier Transform Infrared Spectroscopy (FTIR)

Fourier Transform Infrared Spectroscopy (FTIR) spectra using attenuated total refractance (ATR) mode were recorded at room temperature using Nicolet 6700 (Nicolet Instruments Inc., WI, USA). FTIR spectra were obtained over a range of 450–4000 cm^{-1} at a resolution of 2 cm^{-1}. PLLA spectra were normalized to 868 cm^{-1}, identified as the C–C(O)O stretching mode, which was the least affected peak throughout the whole PLLA degradation process. In the case of PHD spectra were normalized by the CH_2 band at 2930–2940 cm^{-1}. It was not possible to find an accurate peak for normalization of the polymer blends.

2.3.3. Differential scanning calorimetry (DSC)

Differential scanning calorimetry (DSC) analysis of PLLA, PHD, and B50/50 and B90/10 blends was carried out with a Perkin-Elmer Pyris 1 calorimeter (Perkin-Elmer, USA) under nitrogen atmosphere. An initial heating rate of 10 °C/min from −60 °C to 220 °C enabled the data collection after degradation. Then, the sample was cooled down at 10 °C/min up to −60 °C to study the crystallization from the melt state. The crystallinity degree (X_c) was calculated during heating according to equation (2) for each phase of the blend, considering the melting heat for pure crystals of PLLA and PHD, $\Delta H_m{}^\circ{}_{PLLA}$ = 93 J g^{-1} [41] and $\Delta H_m{}^\circ{}_{PCL}$ (PHD soft segments) 148.05 J g^{-1} [42], respectively.

$$X_c\% = ((\Delta H_m - \Delta H_c)/\Delta H_m{}^\circ) * 100 \quad (2)$$

The glass transition (T_g), crystallization (T_c) and melting temperature (T_m); crystallization (ΔH_c) and melting enthalpy (ΔH_m); X_c and the possible changes in these thermal events due to the hydrolytic degradation, were evaluated.

2.3.4. Contact angle

The contact angle of water droplets (5 μL) on dry membrane pieces was measured with a ramé-hart 250 goniometer (ramé-hart Co.; USA) and analyzed by using the ramé-hart software. Fifteen measurements were recorded in 300 s, after 1 min of droplet estabilization. Contact angle of PLLA, PHD, and B50/50 and B90/10 blends was measured as a function of time at each degradation time.

2.3.5. Scanning electron microscopy (SEM)

Morphology of the PLLA, PHD and B50/50 and B90/10 blends tubular structures was observed in a scanning electron microscope (SEM) (JEOL, model JSM-6460LV, Japan) after gold sputtering. Samples were characterized at 0, 1, 16 and 34 weeks, and processed with image processing software (Image Pro Plus; Media Cybernetics Inc., USA). The diameter of 100 nanofibers per sample was measured in order to obtain a meaningful statistical value.

3. Results

3.1. Molecular weight evaluation by GPC and FTIR analysis upon in vitro degradation

Average molecular weights and PI were obtained by GPC as a function of degradation time for the different electrospun vascular grafts (Fig. 1 a–b). As expected, M_n decreased with degradation time. During the first eight weeks, different degradation rates were observed among the studied grafts. Both blended grafts experienced a faster M_n decrease. After this period, all materials showed similar degradation rates. However, the dissimilar degradation rates during the first weeks determined the differences in the molecular weight loss among the materials at 34 weeks.

A total M_n reduction of 59% was observed for PLLA grafts after 34 weeks. On the other hand, PI was maintained around 1.7 during the first 16 weeks, displaying an increase in the last weeks of degradation. PHD exhibited a 63% of M_n loss after 34 weeks, being its degradation rate slightly higher than the obtained for PLLA at the first weeks. A PI around 2 was found along the whole studied degradation period for these grafts.

The presence of new end-groups produced by PLLA or PHD chain cleavage upon degradation was not evidenced by FTIR for these grafts (Fig. 2 a). PLLA showed a characteristic FTIR spectrum, which did not change significantly during degradation, the same

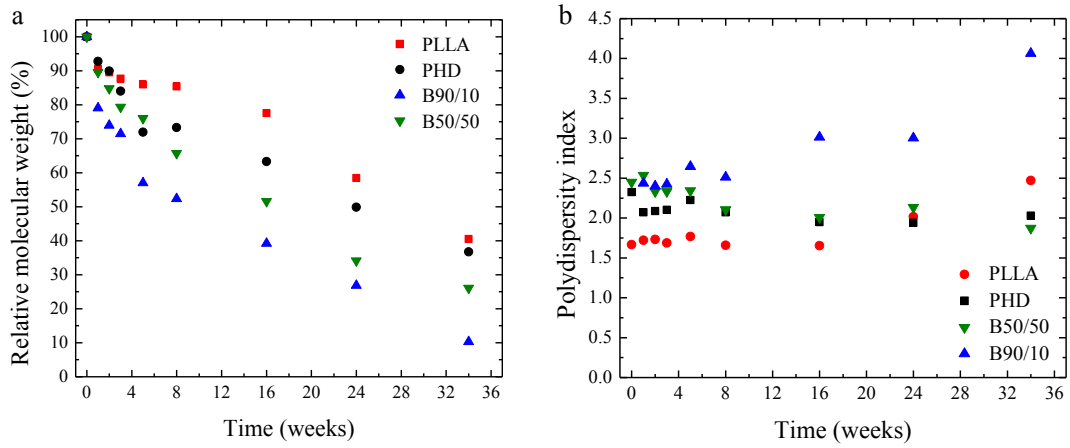

Fig. 1. PLLA, PHD, B90/10 and B50/50 blends electrospun grafts relative molecular weight (%) (a), and PI (b) at different hydrolytic degradation times.

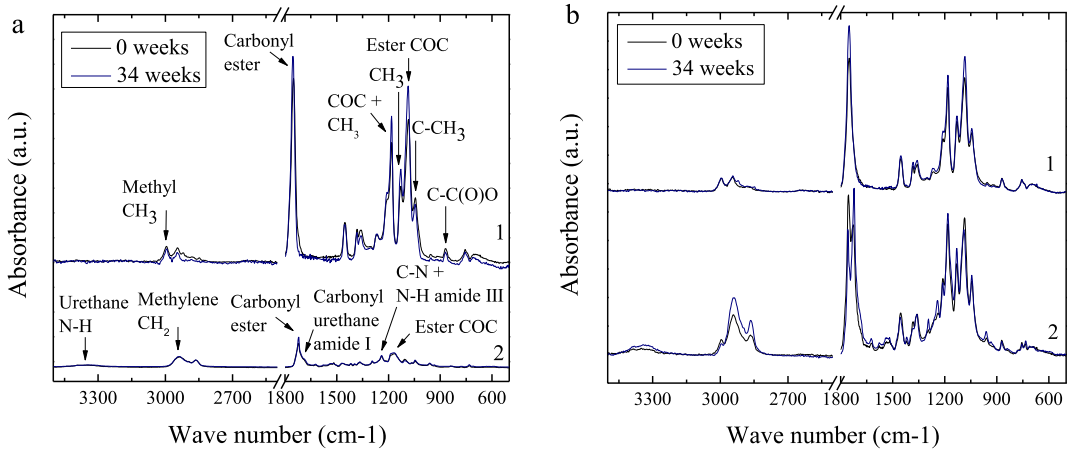

Fig. 2. FTIR spectra for a) PLLA (1) and PHD (2); b) B90/10 (1) and B50/50 (2) blends.

result was observed previously in literature [30]. Although, the intensity of carbonyl peak was modified upon degradation, care must be taken in evaluating this band as the lactic acid carboxyl groups formed on hydrolysis of PLLA have a strong absorbance at 1718 cm^{-1}, and this band overlaps the carbonyl bands centered at 1750 cm^{-1} [43,44]. Consequently, it is not possible to evaluate the kinetics of ester hydrolysis from the changing areas of these composite ester bands without deconvoluting the carbonyl band into its various components [45]. In a similar way, PHD carbonyl band (1720 cm^{-1}) could be overlapped with its acid band at 1715 cm^{-1}, which resulted in an unmodified FTIR spectrum upon degradation.

In comparison with the plain electrospun components, a higher M_n decrease was observed for B50/50 (74%) and B90/10 (90%) blends. This behavior was a consequence of the higher degradation rate observed during the first 8 weeks. Unfortunately, the individual degradation rate of each polymer in the mixture could not be experimentally determined by analyzing the blend elution peak as the one of a pure polymer. On the other hand, the analysis of PI of degraded blends could not be performed due to peaks overlapping hinders further studies. Although FTIR analysis was also performed on the blends (Fig. 2 b), it was not possible to find an accurate peak for normalization for comparison purposes. Again, no new end-groups were detected.

3.2. Thermal properties evaluation by DSC upon in vitro degradation

Tables 1 and 2 present the thermal properties of PLLA and PHD electrospun grafts and their variations during hydrolytic degradation.

Only PLLA exhibited a crystallization event during heating, displaying a decrease in T_c and ΔH_c with degradation time, while T_g and T_m showed minor variations. No crystallization was observed

Table 1
PLLA thermal properties at different degradation times.

Time (weeks)	Heating						Cooling	
	T_g (°C)	T_c (°C)	ΔH_c (J g^{-1})	T_m (°C)	ΔH_m (J g^{-1})	X_c[a] (%)	T_c (°C)	ΔH_c (J g^{-1})
0	63.6	87.2	16.1	154.5	34.3	19.6	–	–
1	64.4	86.1	12.3	154.5	34.0	23.3	–	–
2	64.5	85.9	11.3	154.3	32.7	23.0	–	–
3	63.5	85.5	11.5	154.6	33.9	24.0	–	–
5	63.9	86.1	10.2	155.2	32.6	24.1	–	–
8	63.6	85.5	11.9	154.8	33.3	23.0	–	–
16	62.8	85.0	11.5	154.2	34.1	24.3	–	–
24	64.0	85.3	11.5	155.0	33.9	24.0	–	–
34	62.3	84.6	8.2	155.0	31.8	25.4	–	–

[a] X_c was obtained considering $\Delta H_m = 93$ J g^{-1} for 100% crystalline PLLA [41].

Table 2
PHD thermal properties at different degradation times.

Time (weeks)	Heating				Cooling	
	$T_{g,s}$ (°C)	$T_{m,s}$ (°C)	$\Delta H_{m,s}$ (J g^{-1})	$X_{c,s}$[a] (%)	$T_{c,s}$ (°C)	$\Delta H_{c,s}$ (J g^{-1})
0	−51.6	39.9, 43.9, 57.0	53.5	36.2	−10.38, 27.09	−34.9
1	−55.2	40.3, 48.8	58.7	39.7	−14.03	−30.7
2	−53.8	40.6, 47.6, 49.3	47.1	31.8	−13.14	−33.0
3	−54.4	40.8, 48.8, 50.5	50.8	34.3	−12.91	−35.8
5	−53.7	41.3, 48.8, 50.6	49.8	33.6	−12.95	−30.2
8	−54.5	41.3, 49.8, 51.8	55.7	37.6	−12.57	−29.9
16	−55.3	40.0, 52.3	58.9	39.8	−10.87	−34.9
24	−54.8	39.3, 50.7, 52.5	66.7	45.0	−8.92	−33.9
34	−55.4	39.8, 50.7, 52.5	70.0	47.3	−0.50	−37.7

[a] X_c was calculated considering $\Delta H_m = 148.05$ J g^{-1} for pure high molecular weigth PCL (PHD soft segments) [42].

during cooling. PHD displayed an initial decrease in $T_{g,s}$, remaining essentially constant after the first week. Moreover, PHD exhibited two soft segment melting peaks: the lower temperature peak displayed a decrease in the onset temperature with increasing degradation time, while the higher temperature one melted at lower temperatures. During cooling, PHD soft segments crystallized with a range of crystallization temperatures from 0 to −14 °C. The crystallization enthalpy remained approximately constant with degradation time, showing the same capacity to crystallize of the PHD chains. However, the crystallization temperature moved toward higher values.

Crystallinity was the property exhibiting the most significant changes, displaying a 20%-increase for PLLA and a 10%-increase for PHD during the first week. A further increase in crystallinity was observed with degradation time, being more marked for PHD soft segments since week 5. A decrease in ΔH_m was observed for PLLA at week 34, along with an increase in X_c.

Tables 3 and 4 present the thermal events for B90/10 and B50/50 blends electrospun grafts during hydrolytic degradation. Significant changes in their thermal behavior and thermal properties were appreciated.

Thermal events associated to PHD were only detected in B50/50 during heating. Both blends displayed a decrease in PLLA-related ΔH_c with degradation time, more pronounced for B50/50. While this behavior became more evident at week 34 for B90/10, the exotherm almost disappeared at this degradation time for B50/50. Moreover, PLLA T_c also exhibited variations for both blends, with no apparent trend for B50/50, and a decrease with degradation time for B90/10, but showing higher values than plain PLLA for all degradation times. PLLA-related T_g decreased during degradation for B90/10 blend, and did not follow a trend for B50/50. Moreover, $T_{g,s}$ was only observed for B50/50 grafts and slightly increased with degradation. No changes in PLLA-related T_m were appreciated for B90/10 and B50/50 blends during the degradation process. However, the onset of the melting peak shifted toward lower temperature values with degradation time. This effect was sharper for B50/50 blend, evidencing also the appearance of a second peak at a lower melting temperature at week 34. On the other hand, PHD exhibited a double T_m peak related to soft segment domains ($T_{m,s}$) in B50/50 blend. The lower peak displayed an upshift of about 20 °C after the first week, evidencing no relevant changes with further degradation.

Crystallinity exhibited significant changes with degradation time for both blends. B90/10 and B50/50 blends displayed an increase in PLLA-related crystallinity after the first week of hydrolytic degradation, following the same behavior than PLLA plain grafts. A second increase was observed after week 5 and 3, respectively. B50/50 blend exhibited also a slightly rise in PHD soft segment crystallinity, which became more pronounced after 8 weeks of degradation. Finally, a decrease between 5 and 15% occurred after week 24 for PLLA phase in both blends.

As observed for plain polymers, only PHD crystallized during cooling in both blends. The presence of PHD was evidenced also in the B90/10 grafts. Even more, the ΔH_c at the first weeks of degradation was approximately the same as the value observed for plain PHD grafts, showing the same capability to crystallize. It was reported that even though the molecular weight decreases, the mass remains almost constant during the first 6 months for PHD and PLLA [30,46]. Therefore despite the different degradation rate of each polymer in the blend, the use of the original mass ratio in the calculations introduces only slight variations in the thermal properties. This explains the observed ΔH_c values. At higher degradation times PHD crystallization did not occur, indicating the impossibility of its shorter degraded chains to crystallize. This event was observed earlier for B90/10 grafts which were the ones showing the higher molecular weight loss during degradation.

3.3. Surface properties evaluation by contact angle and SEM upon in vitro degradation

The hydrophilicity and microstructure modification upon degradation were analyzed. Fig. 3 presents the obtained values for the water contact angle of PLLA and PHD grafts. PLLA kept a hydrophobic behavior until week 16 of degradation. A large dispersion in contact angle values was found at the 24th week, which could be attributed to a transition between degradation stages. Finally, at the 34th week the electrospun grafts turned completely hydrophilic. On the other hand, PHD exhibited a hydrophilic behavior during the whole degradation process. After 34 weeks, the contact angles could not be measured due to sample fragmentation and lack of mechanical integrity.

Table 3
B90/10 blend thermal properties at different degradation times.

Time (weeks)	Heating						Cooling	
	T_g PLLA (°C)	T_c PLLA (°C)	ΔH_c PLLA (J g^{-1})	T_m PLLA (°C)	ΔH_m PLLA (J g^{-1})	X_c PLLA[a] (%)	$T_{c,s}$ PHD (°C)	$\Delta H_{c,s}$ PHD (J g^{-1})
0	61	90.2	14.1	151.6, 154.4	31.2	18.3	−9.56	−38.1
1	61.5	97.3	12.0	155.3	35.0	24.8	−6.75	−30.2
2	62.4	91.0	13.5	154.7	39.3	27.8	−5.72	−33.4
3	61.4	90.9	10.4	154.9	34.1	25.5	−5.25	−34.9
5	61.0	92.6	11.9	155.8	34.8	24.7	−6.13	−30.8
8	59.5	92.9	10.7	155.8	35.4	26.6	−6.08	−31.5
16	58.7	88.6	10.6	155.2	38.7	30.2	–	–
24	54.5	87.3	12.4	155.4	46.1	36.3	–	–
34	44.4	87.6	6.7	155.0	38.3	34.0	–	–

[a] X_c was obtained considering $\Delta H_m = 93$ J g^{-1} for 100% crystalline PLLA [41].

Table 4
B50/50 blend thermal properties at different degradation times.

Time (weeks)	Heating										Cooling	
	T_g PLLA (°C)	$T_{g,s}$ PHD (°C)	T_c PLLA (°C)	ΔH_c PLLA (J g^{-1})	T_m PLLA (°C)	ΔH_m PLLA (J g^{-1})	X_c PLLA[a] (%)	$T_{m,s}$ PHD (°C)	$\Delta H_{m,s}$ PHD (J g^{-1})	X_c PHD[b] (%)	$T_{c,s}$ PHD (°C)	$\Delta H_{c,s}$ PHD (J g^{-1})
0	55	−59	83.4	9.1	153.7	33.6	26.4	25.4, 52.7	18.5	16.4	−11.17	−26.8
1	59.5	−56.1	80.0, 82.0	2.8	153.5	44.6	45.0	43.3, 56.1	25.92	17.51	−13.45	−29.8
2	57.9	−55.3	80.0, 81.9	2.6	154.0	43.3	43.7	42.4, 46.3	19.53	13.19	−12.21	−34.0
3	63.8	–	86.6	7.0	154.9	40.5	36.0	42.8, 51.7	26.68	18.02	−11.45	−38.2
5	59.6	−54.8	81.0, 82.2, 83.2	2.0	154.3	43.9	45.0	42.3, 48.9	25.76	17.40	−9.88	−34.0
8	57.2	–	79.8	1.3	154.6	46.5	48.6	42.0, 48.0	21.92	14.80	−7.16	−39.0
16	60.1	–	84.9	0.3	153.6	50.1	53.6	42.3, 49.5	36.85	24.89	−5.34	−38.1
24	57.9	–	–	–	152.7	52.4	56.4	38.8, 47.7	44.37	29.97	−9.92	−3.0
34	58.5	–	–	–	139.6, 149.9	45.0	48.4	38.8, 49.8	49.85	33.67	–	–

[a] X_c was obtained considering $\Delta H_m = 93$ J g^{-1} for 100% crystalline PLLA [41].
[b] X_c was calculated considering $\Delta H_m = 148.05$ J g^{-1} for pure high molecular weigth PCL (PHD soft segments) [42].

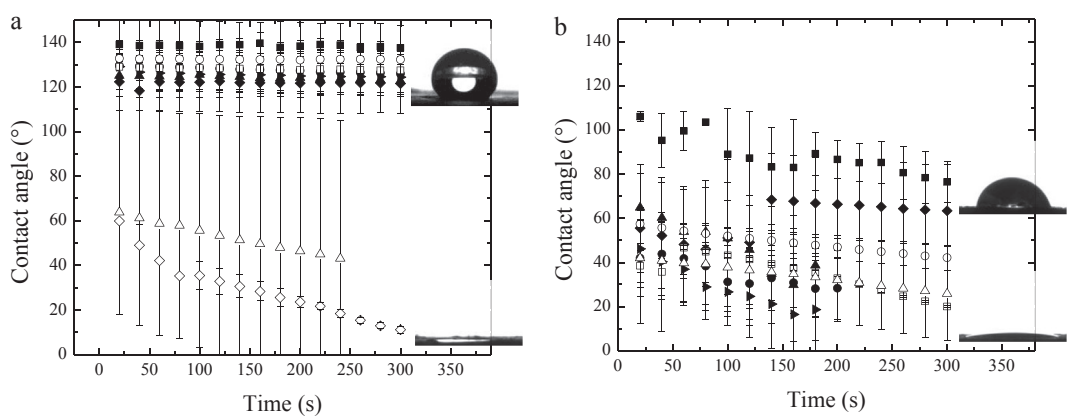

Fig. 3. Contact angle measurements as a function of time for a) PLLA and b) PHD electrospun vascular grafts at 0 (■), 1 (●), 2 (▲), 3 (◆), 5 (►), 8 (□), 16 (○), 24 (Δ) and 34 (◊) degradation weeks.

B90/10 and B50/50 blends displayed an increase in hydrophilicity with degradation time (Fig. 4). Indeed, the water droplet was completely absorbed before 5 min for all the degraded samples. For B90/10 blend, the contact angle decreased abruptly to a value around 20° after the first week, and the water droplet was absorbed during the stabilization time since week 8. For B50/50 blend, the contact angle decreased less steeply with degradation time until reaching a value around 30° and remained constant from the third week of degradation on. After 24 and 34 weeks, the water droplet was immediately absorbed.

SEM micrographs display the nanofibrous morphology (Fig. 5), and Table 5 shows the fiber mean diameter upon degradation for all grafts. No significant differences were detected in the fiber size for PLLA nor for B90/10 grafts ($p < 0.05$) after 34 weeks. On the other hand, PHD and B50/50 grafts showed a significant decrease in fiber diameter with degradation time ($p < 0.05$), being more pronounced

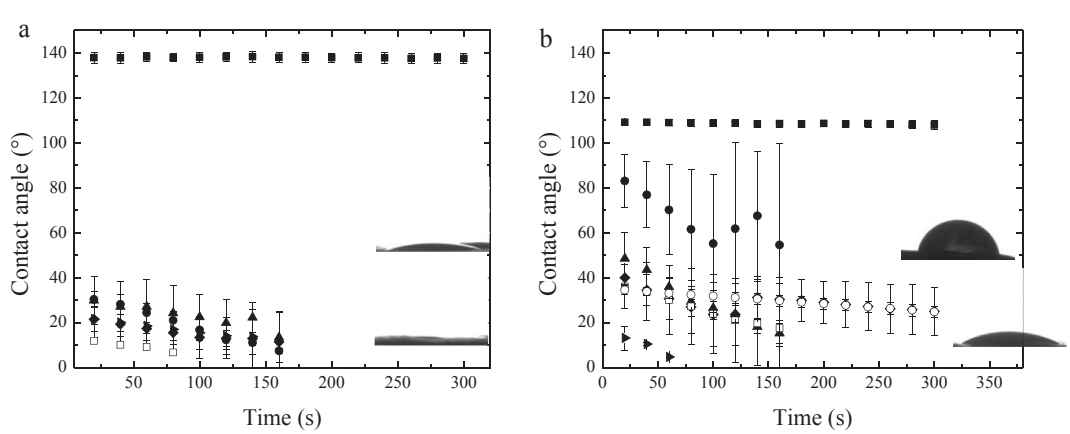

Fig. 4. Contact angle measurements as a function of time for a) B90/10 and b) B50/50 blends electrospun vascular grafts at 0 (■), 1 (●), 2 (▲), 3 (◆), 5 (►), 8 (□) and 16 (○) degradation weeks.

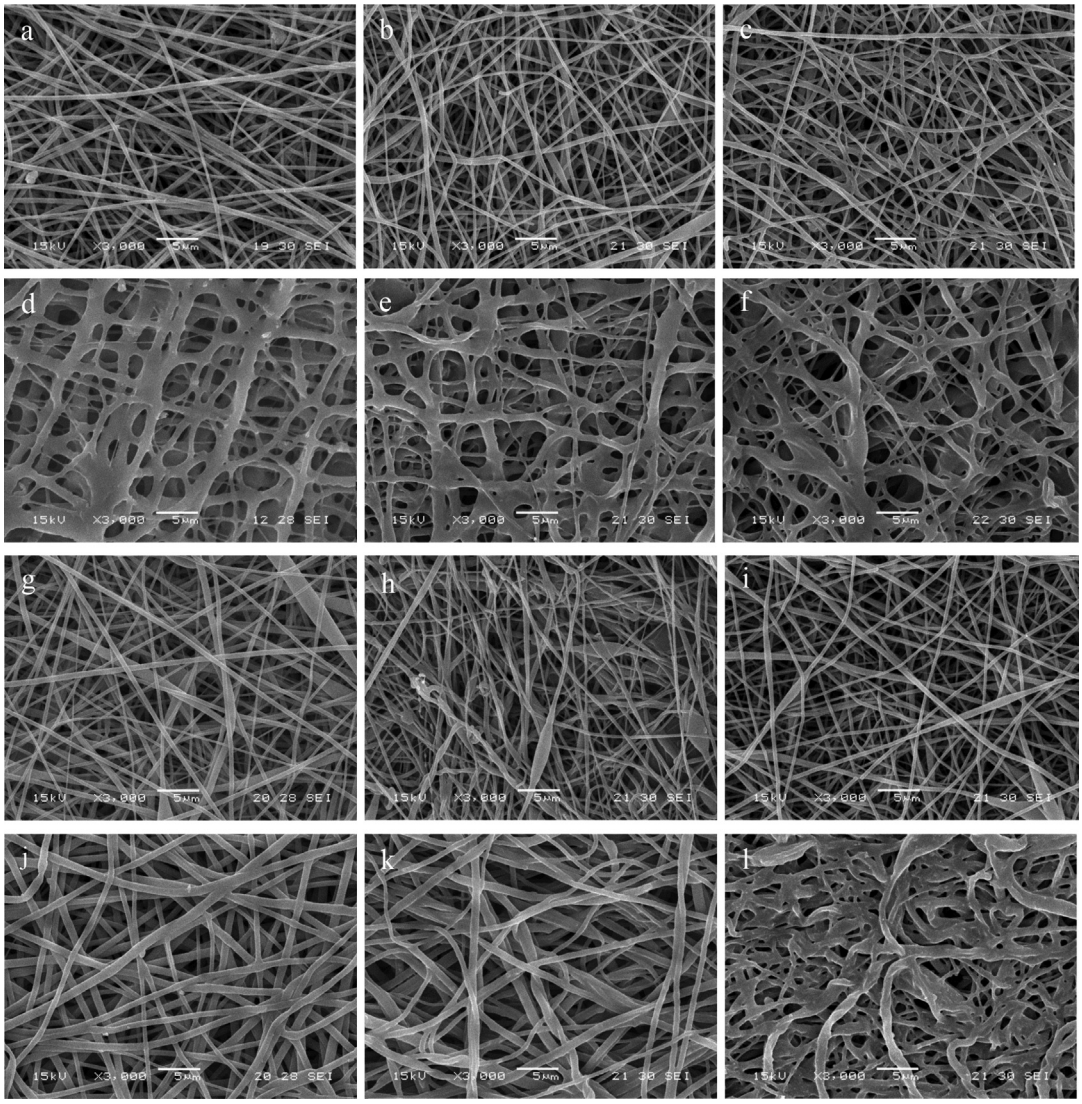

Fig. 5. SEM micrographs for PLLA (a, b, c), PHD (d, e, f), B90/10(g, h, i) and B50/50 (j, k, l) blends electrospun grafts as a function of degradation time, at 0 (a, d, g, j), 16 (b, e, h, k) and 34 (c, f, i, l) weeks.

Table 5
Mean fiber diameters for the electrospun grafts after 0, 1, 16 and 34 weeks of degradation.

Samples	Mean diameter (nm)			
	0 week	1 week	16 weeks	34 weeks
PLLA	383 ± 103	375 ± 138	390 ± 119	407 ± 118
PHD	687 ± 290[b,c]	641 ± 413	515 ± 252	558 ± 284
B90/10	410 ± 124[a,b]	463 ± 170	359 ± 122[f]	425 ± 129
B50/50	754 ± 210[a,b,c]	590 ± 232[d]	619 ± 199[f]	532 ± 235

[a,b,c] significant differences ($p < 0.05$) between the measured diameter before and after 1, 16 and 34 weeks of degradation, respectively.
[d,e] significant differences ($p < 0.05$) between the measured diameter at 1 week respect 16 and 34 weeks.
[f] significant differences ($p < 0.05$) between the measured diameter at 16 weeks respect 34 weeks.

for PHD after 16 and 34 weeks. Both PHD and B50/50 samples broke into pieces during manipulation and showed lack of mechanical stability in the last weeks of the degradation study, consistently with the structural weakening caused by the fibers thinning. Besides the significant change observed in PHD and B50/50 fiber diameter, the samples maintained their nanofibrous structure.

4. Discussion

The degradation mechanism for electrospun PLLA is proposed in Fig. 6 a. PLLA is believed to undergo different stages of hydrolytic degradation. Besides, Zong et al. proposed a thermally induced crystallization step as a previous stage in the electrospun PLGA degradation mechanism, caused by an annealing process due to the *in vitro* degradation temperature proximity to the polymer T_g [19]. A similar thermally induced stage is proposed for PLLA grafts, where crystallization from amorphous domains in PLLA nanofibers occurs and lamellar stacks are formed. Afterwards, it is known that polyesters degradation begins with water diffusion into the amorphous regions, leading to random hydrolytic cleavage of ester bonds. Mobility of polymer chains within the amorphous regions increases after chain scission [18–20], cleavage-induced crystallization occurs and thinner more defective crystals are formed.

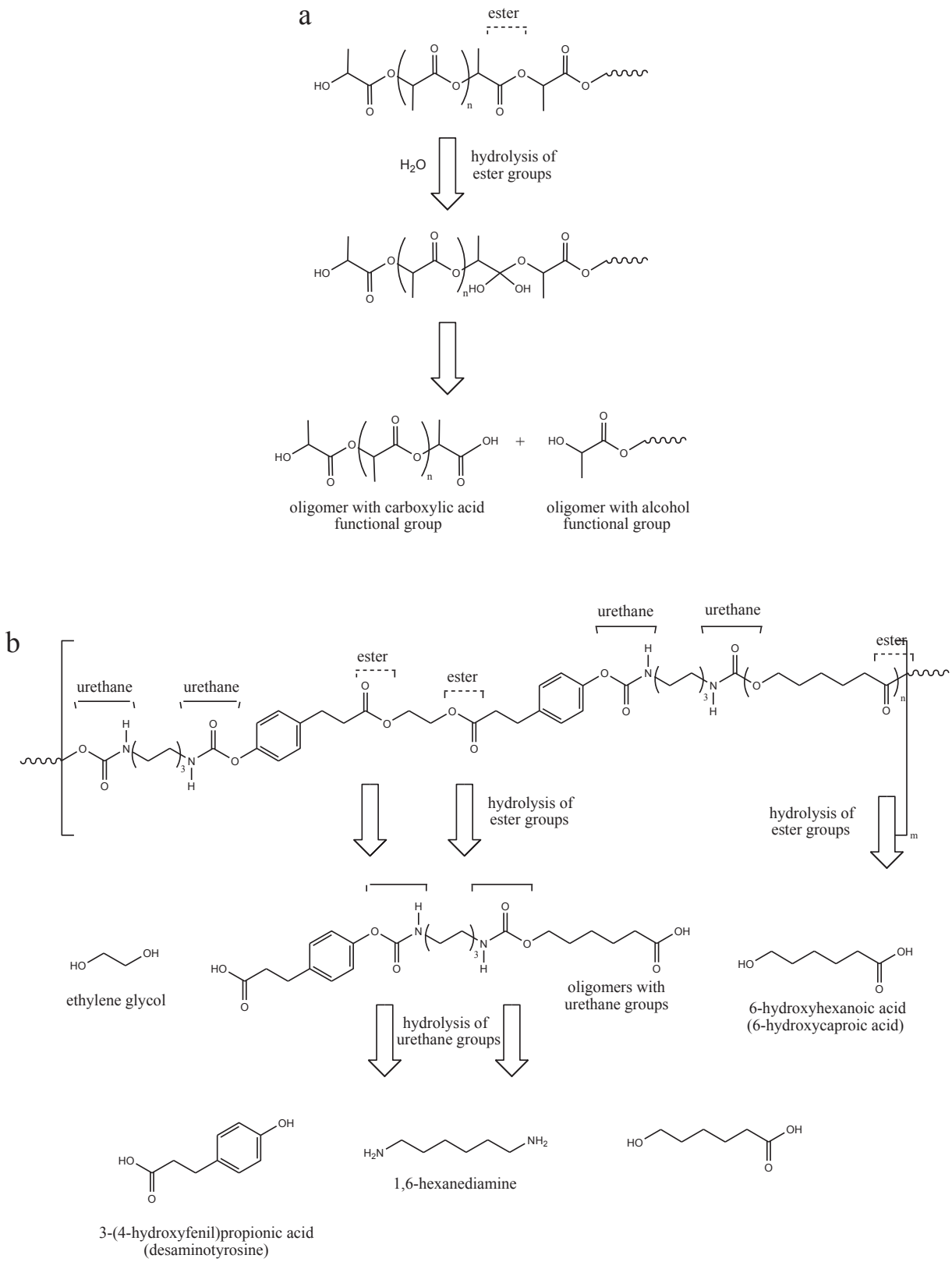

Fig. 6. a) PLLA and b) PHD possible scission sites and degradation byproducts.

Though the molecular weight drops at this stage, the shorter chains generated are still hydrophobic and insoluble. Thus, they could remain inside the nanofibrous structure and no appreciable reduction in the sample mass takes place, as reported in the literature [30,46,47]. Later, the increase of acid end-groups in the nanofibrous structure due to the degradation process accelerates

the decrease in molecular weight. An autocatalytic effect takes place, resulting in shorter and more hydrophilic polymeric chains. Finally, the crystalline regions become susceptible to hydrolysis.

The first stage of thermally induced crystallization was evidenced by an increase in crystallinity, and the initial degradation was indicated by a decrease in molecular weight, both at the first week. It is unlikely that new crystals had been formed due to the cleavage of amorphous domains after one week under hydrolytic conditions. Moreover, the fact that ΔH_c decreased while ΔH_m remained constant, suggests that annealing actually takes place. The low relative molecular weight decrease agrees with this hypothesis, suggesting additionally an early chain scission in amorphous regions. Therefore, an annealing process favored by an aqueous medium could be responsible for the observed crystallinity increase in PLLA nanofibers. The hydrolysis of ester bonds at amorphous regions continued in the following weeks. The hydrophobic nature of the grafts evidenced by contact angle until week 16, together with the fact that no change in the medium pH was detected, could indicate that lower molecular weight chains with acidic end-groups may remain trapped in the nanofibrous 3D structure. Therefore, it is believed that an autocatalytic effect occurred, leading to a faster molecular weight reduction. Indeed, the lack of alteration of the nanofibrous structure after 34 weeks suggests that the hydrolytic *in vitro* degradation process mainly took place through acidic catalysis mediated by these shorter chains inside the fibrous structure. The continuous increase in PLLA crystallinity is due to crystallization of the more mobile shorter chains from partially degraded amorphous regions. At advanced assay times, the beginning of chain scission at the crystalline regions can be identified by a drop of ΔH_m. However, an increase in X_c suggests that crystallization of the partially degraded amorphous domains takes place simultaneously. Finally, the decrease in contact angle values at 24th and 34th weeks indicates the formation of short hydrophilic chains in agreement with the presence of oligomers detected by GPC. Despite the evidences of PLLA chain cleavage upon degradation, no significant acidic functional groups could be detected in the FTIR spectra (probably due to their low content in the sample surface), consistent with the proposed acidic catalysis inside the fibrous structure.

PHD degradation is also produced by hydrolytic mechanisms, involving ester groups from PCL soft segment and chain extender, and urethane groups that connect soft-to-hard segments. Fig. 6 b shows the possible scission sites and degradation byproducts. Even though the scission sites differ from PLLA ones, the degradation stages in PHD are similar.

The first stage of thermally induced crystallization previously described for PLLA seems to have taken place to a lesser extent in this case. In spite of the proximity of the *in vitro* degradation temperature to $T_{m,s}$, hydrogen bonded hard segments may limit chain mobility, displaying PHD a lower capacity than PLLA to go on annealing. PHD presented a slightly higher molecular weight decrease and a faster degradation rate than PLLA. The presence of polar functional groups in PHD led to a hydrophilic behavior during the whole degradation process, what could have been responsible for a better water accessibility inside the nanofibers, and therefore a higher chain scission rate. Moreover, chain cleavage occurred in the amorphous regions, leading to an increase in chain mobility and favoring a later crystallization. In fact, thermal analysis showed an increase in PHD soft domain crystallinity with degradation time. In a posterior stage, shorter insoluble chains with acid end-groups accelerated the degradation process. The maintenance of the nanofibrous structure and stable pH of the degradation medium could indicate an autocatalytic stage. No signs of degradation at crystalline regions were detected. Even though the percentage of M_n loss was significant, PHD soft segments chains maintained their capacity to crystallize during cooling. SEM analysis showed a significant decrease in the fibers mean diameter after 16 weeks of degradation, indicating surface erosion and possible diffusion of some more hydrophilic shorter chains into the degradative medium. This was consistent with the structural weakening observed during sample manipulation and the large fluctuation of contact angle values.

The higher degradation rate observed for B90/10 and B50/50 compared with the plain grafts could be attributed to the blend formulation. It was reported that for polyester blend systems the degradation rate of each component is modified by the presence of the other [8]. In this way, the slower degrading polymer increases its rate by blending with another with a higher degradation rate, while the latter degrades slower due to the presence of the first. In more recent works it was observed that the degradation rate of electrospun polymers was increased by blending with a faster degradable polymer [10,48]. Chung et al. proved the accelerated degradation of PCL when blended with a PGA-PCL-PGA triblock copolymer [10]. In our system, a similar synergistic outcome was produced by blending, which led to a higher reduction in the apparent molecular weight for both studied blends respect to the plain polymers. It is suggested that this phenomenon occurs since the faster degrading PHD accelerates the degradation process for PLLA and itself in the blend. The local acidic environment produced by insoluble cleaved chains, mainly from the faster degrading PHD, exposes PLLA to an earlier and more pronounced degradation. In the same way, this acidic medium (mainly generated from PHD degradation) catalyzes not only PHD further degradation but also PLLA degradation in the blend. This hypothesis could explain the higher molecular weight reduction seen for both blends.

It is suggested that differences in crystallinity and hydrophilicity observed due to blending could also affect the degradative behavior of each component, as reported in previous studies [36]. In this way, B50/50 blend grafts presented significantly lower soft domain crystallinity than PHD grafts, together with a higher hydrophilicity, which led to a faster degradation than plain polymer grafts. Compared with B90/10 blend, B50/50 blend grafts showed a lower degradation rate, probably due to its higher PLLA-related crystallinity and less hydrophilic behavior. On the other hand, B90/10 blend grafts presented lower initial PLLA-related crystallinity than B50/50 grafts, which added to a high hydrophilicity, could have led to the highest degradation rate among all the studied grafts. In addition, the presence of amorphous PHD could have enhanced water permeation, favoring the degradation process.

The higher hydrophilicity of the electrospun blends with respect to the plain polymers was in agreement with the higher M_n decrease detected. In fact, B90/10 presented the lowest contact angle at the first week, consistently with its fastest degradation. While crystallinity continuously increased for the plain polymers grafts during degradation, a decrease at 34 weeks was observed for the PLLA semicrystalline regions in both blends. This effect suggests that PLLA enters in the final degradation stage when blended, consistently with the higher M_n diminution seen by GPC. The loss of PHD soft segments crystallization in the blends during cooling at advanced degradation times, indicates the impossibility of shorter more defectuos chains to crystallize. This behavior was not observed for plain PHD grafts, suggesting that PHD also suffer a higher degradation when blended.

5. Conclusions

PLLA, PHD, and their blends presented a molecular weight decrease of 60–90% after 34 weeks of hydrolytic degradation. The blends displayed a higher M_n decrease than plain PLLA and PHD grafts. The combined effects of low initial crystallinity and high

hydrophilicity along with a synergetic outcome produced by blending led to a faster degradation rate. All grafts exhibited an increase in crystallinity with degradation time, but a further decrease for PLLA-related X_c due to crystalline regions degradation was only observed for the blends at advanced degradation times. PHD phase also suffered a higher degradation when blended, evidenced by the impossibility to crystallize during cooling at advanced degradation times. Moreover, both blends presented a similar apparent M_n after 34 weeks. This fact suggests that a bilayered vascular graft composed by inner and outer layers made of B50/50 and B90/10, respectively, degrades as a whole at a rather uniform rate, which is ideal for the desired application.

Tissue-engineering applications require coordination between degradation and tissue regeneration rates. The fact that an *in vitro* degradation process is slower than an *in vivo* one indicates that the use of *in vitro* regeneration times for a vascular graft are required for comparison purposes. This could be approximated as the time required to produce a vascular graft through the cell-sheet technique, which was estimated to take place in around 8 weeks [49]. Both B50/50 and B90/10 blends underwent a significant molecular weight loss after 34 weeks of *in vitro* degradation and became stiffer and fragmented between 16 and 24 weeks. Considering that these structures will be subjected to cyclic mechanical solicitations, the grafts should maintain their integrity until the regenerating tissue is able to withstand the pressure by its own. It could be concluded that the *in vitro* regeneration time agrees with the degradation time at which the grafts maintain their structural integrity.

Overall, the obtained results present a very promising perspective regarding the matching of regeneration and degradation processes. This finding makes them encouraging for future *in vivo* studies and their actual performance as degradable small-diameter vascular constructs.

Acknowledgements

F.M.B. thanks to CONICET for the postdoctoral scholarship. This work was supported by the Argentinean National Agency of Scientific and Technological Promotion (PICT 224), and CONICET (PIP 0089).

References

[1] A. Kramschuster, L.-S. Turng, 17-Fabrication of Tissue Engineering Scaffolds, in Handbook of Biopolymers and Biodegradable Plastics, in: S. Ebnesajjad (Ed.), William Andrew Publishing, Boston, 2013, pp. 427–446.
[2] F.J. O'Brien, Biomaterials & scaffolds for tissue engineering, Mater. Today 14 (3) (2011) 88–95.
[3] L.S. Nair, C.T. Laurencin, Biodegradable polymers as biomaterials, Prog. Polym. Sci. 32 (8–9) (2007) 762–798.
[4] R.M. Ginde, R.K. Gupta, In vitro chemical degradation of poly(glycolic acid) pellets and fibers, J. Appl. Polym. Sci. 33 (7) (1987) 2411–2429.
[5] C.C. Chu, An in-vitro study of the effect of buffer on the degradation of poly(glycolic acid) sutures, J. Biomed. Mater. Res. 15 (1) (1981) 19–27.
[6] M. Mochizuki, M. Hirami, Structural effects on the biodegradation of aliphatic polyesters, Polym. Adv. Technol. 8 (4) (1997) 203–209.
[7] M.-H. Huang, et al., Degradation characteristics of poly(ε-caprolactone)-based copolymers and blends, J. Appl. Polym. Sci. 102 (2) (2006) 1681–1687.
[8] Y. Cha, C.G. Pitt, The biodegradability of polyester blends, Biomaterials 11 (2) (1990) 108–112.
[9] M. Hiljanen-Vainio, et al., Modification of poly(L-lactides) by blending: mechanical and hydrolytic behavior, Macromol. Chem. Phys. 197 (4) (1996) 1503–1523.
[10] A.S. Chung, et al., Lamellar stack formation and degradative behaviors of hydrolytically degraded poly(ε-caprolactone) and poly(glycolide-ε-caprolactone) blended fibers, J. Biomed. Mater. Res. Part B Appl. Biomater. 100B (1) (2012) 274–284.
[11] H. Tsuji, Y. Ikada, Blends of aliphatic polyesters. I. Physical properties and morphologies of solution-cast blends from poly(DL-lactide) and poly(ε-caprolactone), J. Appl. Polym. Sci. 60 (13) (1996) 2367–2375.
[12] L. Ghasemi-Mobarakeh, et al., Electrospun poly(ε-caprolactone)/gelatin nanofibrous scaffolds for nerve tissue engineering, Biomaterials 29 (34) (2008) 4532–4539.
[13] J.J. Stankus, J. Guan, W.R. Wagner, Fabrication of biodegradable elastomeric scaffolds with sub-micron morphologies, J. Biomed. Mater. Res. Part A 70A (4) (2004) 603–614.
[14] S.J. Lee, et al., Development of a composite vascular scaffolding system that withstands physiological vascular conditions, Biomaterials 29 (19) (2008) 2891–2898.
[15] W. Amass, A. Amass, B. Tighe, A review of biodegradable polymers: uses, current developments in the synthesis and characterization of biodegradable polyesters, blends of biodegradable polymers and recent advances in biodegradation studies, Polym. Int. 47 (2) (1998) 89–144.
[16] B. Gupta, N. Revagade, J. Hilborn, Poly(lactic acid) fiber: An overview, Prog. Polym. Sci. 32 (4) (2007) 455–482.
[17] D. Suarez Bagnasco, et al., Elasticity assessment of electrospun nanofibrous vascular grafts: a comparison with femoral ovine arteries, Mater. Sci. Eng. C 45 (0) (2014) 446–454.
[18] K. Kim, et al., Control of degradation rate and hydrophilicity in electrospun non-woven poly(d,l-lactide) nanofiber scaffolds for biomedical applications, Biomaterials 24 (27) (2003) 4977–4985.
[19] X. Zong, et al., Structure and morphology changes during in vitro degradation of electrospun poly(glycolide-co-lactide) nanofiber membrane, Biomacromolecules 4 (2) (2003) 416–423.
[20] M.C. Araque-Monrós, et al., Study of the degradation of a new PLA braided biomaterial in buffer phosphate saline, basic and acid media, intended for the regeneration of tendons and ligaments, Polym. Degrad. Stab. 98 (9) (2013) 1563–1570.
[21] L.A. Gaona, et al., Hydrolytic degradation of PLLA/PCL microporous membranes prepared by freeze extraction, Polym. Degrad. Stab. 97 (9) (2012) 1621–1632.
[22] R.J. Zdrahala, I.J. Zdrahala, Biomedical applications of polyurethanes: a review of past promises, present realities, and a vibrant future, J. Biomater. Appl. 14 (1) (1999) 67–90.
[23] S.A. Guelcher, Biodegradable polyurethanes: synthesis and applications in regenerative medicine, Tissue Eng. Part B Rev. 14 (1) (2008) 3–17.
[24] G.A. Abraham, P.M. Frontini, T.R. Cuadrado, Physical and mechanical behavior of sterilized biomedical segmented polyurethanes, J. Appl. Polym. Sci. 65 (6) (1997) 1193–1203.
[25] P.C. Caracciolo, F. Buffa, G.A. Abraham, Effect of the hard segment chemistry and structure on the thermal and mechanical properties of novel biomedical segmented poly(esterurethanes), J. Mater. Sci. Mater. Med. 20 (1) (2009) 145–155.
[26] J.P. Santerre, et al., Understanding the biodegradation of polyurethanes: from classical implants to tissue engineering materials, Biomaterials 26 (35) (2005) 7457–7470.
[27] X. Zong, et al., Structure and process relationship of electrospun bioabsorbable nanofiber membranes, Polymer 43 (16) (2002) 4403–4412.
[28] M.S. Rizvi, et al., Mathematical model of mechanical behavior of micro/nanofibrous materials designed for extracellular matrix substitutes, Acta Biomater. 8 (11) (2012) 4111–4122.
[29] C.-L. Pai, M.C. Boyce, G.C. Rutledge, On the importance of fiber curvature to the elastic moduli of electrospun nonwoven fiber meshes, Polymer 52 (26) (2011) 6126–6133.
[30] J.C. Dias, et al., Influence of fiber diameter and crystallinity on the stability of electrospun poly(l-lactic acid) membranes to hydrolytic degradation, Polym. Test. 31 (6) (2012) 770–776.
[31] S. Baudis, et al., Hard-block degradable thermoplastic urethane-elastomers for electrospun vascular prostheses, J. Polym. Sci. Part A Polym. Chem. 50 (7) (2012) 1272–1280.
[32] H.N. Patel, et al., Fibro-porous poliglecaprone/polycaprolactone conduits: synergistic effect of composition and in vitro degradation on mechanical properties, Polym. Int. 64 (4) (2015) 547–555.
[33] J.A. Henry, et al., Characterization of a slowly degrading biodegradable polyesterurethane for tissue engineering scaffolds, J. Biomed. Mater. Res. Part A 82A (3) (2007) 669–679.
[34] N. Bolgen, et al., In vitro and in vivo degradation of non-woven materials made of poly(epsilon-caprolactone) nanofibers prepared by electrospinning under different conditions, J. Biomater. Sci. Polym. Ed. 16 (12) (2005) 1537–1555.
[35] S.R. Bhattarai, et al., Novel biodegradable electrospun membrane: scaffold for tissue engineering, Biomaterials 25 (13) (2004) 2595–2602.
[36] F. Montini Ballarin, et al., Optimization of poly(l-lactic acid)/segmented polyurethane electrospinning process for the production of bilayered small-diameter nanofibrous tubular structures, Mater. Sci. Eng. C 42 (0) (2014) 489–499.
[37] R.L. Armentano, et al., Similarities of arterial collagen pressure-diameter relationship in ovine femoral arteries and PLLA vascular grafts, in: Engineering in Medicine and Biology Society (EMBC), 2014 36th Annual International Conference of the IEEE, 2014.
[38] F. Montini Ballarin, et al., Mechanical behaviour of bilayered small-diameter nanofibrous structures as biomimetic vascular grafts, J. Mech. Behav. Biomed. Mater. 60 (July 2016) 220–233.
[39] D. Suarez-Bagnasco, et al., in: A. Braidot, A. Hadad (Eds.), An in Vitro Set up for the Assessment of Electrospun Nanofibrous Vascular Grafts, in VI Latin American Congress on Biomedical Engineering CLAIB 2014, Paraná, Argentina

29, 30 & 31 October 2014, Springer International Publishing, 2015, pp. 144–147.
[40] R.L. Armentano, et al., High pressure assessment of bilayered electrospun vascular grafts by means of an Electroforce Biodynamic System®, in: Engineering in Medicine and Biology Society (EMBC), 2015 37th Annual International Conference of the IEEE, 2015.
[41] E.W. Fischer, H. Sterzel, G. Wegner, Investigation of the structure of solution grown crystals of lactide copolymers by means of chemical reactions, Kolloid-Zeitschrift und Zeitschrift für Polymere 251 (11) (1973) 980–990.
[42] D.W. Van Krevelen, K. Te Nijenhuis, in: D.W. van Krevelen, K.T. Nijenhuis (Eds.), Chapter 5-Calorimetric Properties, in Properties of Polymers, fourth ed., Elsevier, Amsterdam, 2009, pp. 109–128.
[43] G. Cassanas, et al., Vibrational spectra of lactic acid and lactates, J. Raman Spectrosc. 22 (7) (1991) 409–413.
[44] G. Kister, G. Cassanas, M. Vert, Effects of morphology, conformation and configuration on the IR and Raman spectra of various poly(lactic acid)s, Polymer 39 (2) (1998) 267–273.
[45] D.K. Wang, et al., FT-IR characterization and hydrolysis of PLA-PEG-PLA based copolyester hydrogels with short PLA segments and a cytocompatibility study, J. Polym. Sci. Part A Polym. Chem. 51 (24) (2013) 5163–5176.
[46] P.C. Caracciolo, et al., Biodegradable polyurethanes: comparative study of electrospun scaffolds and films, J. Appl. Polym. Sci. 121 (6) (2011) 3292–3299.
[47] A.C. Vieira, et al., Mechanical study of PLA–PCL fibers during in vitro degradation, J. Mech. Behav. Biomed. Mater. 4 (3) (2011) 451–460.
[48] A.S. Asran, et al., Nanofibers from blends of polyvinyl alcohol and polyhydroxy butyrate as potential scaffold material for tissue engineering of skin, Biomacromolecules 11 (12) (2010) 3413–3421.
[49] C.E. Fernandez, et al., Biological and engineering design considerations for vascular tissue engineered blood vessels (TEBVs), Curr. Opin. Chem. Eng. 3 (2014) 83–90.